I.M. BOLESTA,[1] I.N. ROVETSKII,[1] Z.M. YAREMKO,[2] I.D. KARBOVNYK,[1]
S.R. VELGOSH,[1] M.V. PARTYKA,[3] N.V. GLOSKOVSKAYA,[4] V.M. LESIVTSIV[1]

[1] Ivan Franko National University of Lviv, Faculty of Electronics,
  Chair of Radiophysics and Computer Technologies
  (107, Gen. Tarnavs'kyi Str., Lviv 79017, Ukraine; e-mail: bolesta@electronics.lnu.edu.ua)
[2] Ivan Franko National University of Lviv, Department of Life Safety
  (41, Doroshenko Str., Lviv 79000, Ukraine)
[3] Ivan Franko National University of Lviv, Faculty of Physics, Chair of Solid State Physics
  (50, Dragomnov Str., Lviv 79005, Ukraine)
[4] Bogolyubov Institute for Theoretical Physics, Nat. Acad. of Sci. of Ukraine
  (14-b, Metrolohichna Str., Kyiv, 03680, Ukraine)

PACS 81.07.-b, 87.64.Dz

ON THE MECHANISM OF NANOSTRUCTURE GROWTH ON THE SURFACE OF CdI$_2$ CRYSTALS

Atomic force microscopy studies of the dynamics of the nanostructure formation on a van der Waals surface of CdI$_2$ crystals during aging in air environment under near-equilibrium thermodynamic conditions have been carried out. The nanostructure growth process is found to consist of three stages. At the first stage, there appear nano-sized pores due to the lattice dissolution at the outcrops of screw dislocations or other structural defects. At the second stage, the cone-shaped nanoclusters arise and grow in those nano-sized pores. At the third stage, the nanoclusters coagulate. The growth kinetics of cone-shaped nanoclusters is described by a diffusion model based on the interdiffusion approximation for the components. The growth rate of nanoclusters is shown to depend on the time evolution of the concentration gradient of Cd^{2+} ions in the near-reaction zone.

K e y w o r d s: atomic force microscopy, van der Waals surface, nanopores, nanoclusters, diffusion.

1. Introduction

The research of nanostructures aimed at searching the materials with new functional characteristics to be used in modern devices and micro- and nanoelectronic systems is a challenging task for the modern physics of semiconductors and insulators. In this aspect, promising are layered crystals, the surface of which contains extended, atomically smooth sections with a low density of dangling bonds, which are called van der Waals surfaces (VdW surfaces). This feature is responsible for their application as substrates for the formation of molecular, organic, and metallic nanostructures, as well as for the fabrication of heterostructures using the method of "noncoherent VdW epitaxy" as natural nanorelief standards in the nano-object metrology [1–4].

At present, the formation and properties of nano-dimensional structures in layered crystals of A^{III}B^{VI} group – GaSe, InSe, and In$_x$Se$_{1-x}$ alloys – are intensively studied [5–8]. However, similar researches are scarcely known for wide-gap halogenides of the MX$_2$ type with layered structure.

The results of microscopic investigations dealing with the surface of layered CdI$_2$ crystals grown up from aqueous solutions were discussed in a number of works [9–13]. Using the methods of optical, tunnel electron (TEM), and scanning electron (SEM) microscopies, the new elements of growth spirals were revealed, which were formed on the basis of faces (0001) of CdI$_2$; namely, these are substeps with a height that is equal to or multiple of the c-period of the crystal structure. The horizontal distance between the steps is a multiple of the lattice a-parameter [9–11]. A mismatch between the height of a growth spiral and the c-period of the lattice was also found, which is associated with the interaction between non-compensated

bonds on the dangling layers (steps) I–Cd–I and the crystal surface and gives rise to a reduction in the thickness of the structural I–Cd–I layer from 0.343 to 0.310 nm [12].

The atomic force microscopy (AFM) study of the surface morphology of CdI_2 crystals grown from an aqueous solution revealed linear steps (terraces), troughs, and islands. The CdI_2 surface was atomically smooth between those elements: the relief inhomogeneity amounted to 10.2 and 4.7 Å [13].

Using the electron microscopy methods, the formation of nanostructures was revealed. Their growth occurred owing to the recrystallization of an evaporated material under the irradiation of a CdI_2 powder with an electron beam. The formed particles are mainly metallic, because the Cd : I ratio for them amounts to 2 : 1, whereas this ratio for stoichiometric compounds equals 1.5 : 2 [14]. Metallic clusters were also revealed in non-stoichiometric CdI_2–Cd crystals [15]. The formation of microtubes was detected in micropores of doped CdI_2–BiI_3 crystals [16].

The practical application of CdI_2 crystals in the scintillation equipment as elements for the optical information recording [17] explains the importance of the formation process research and the analysis of the morphometric parameters of nanostructures formed on the VdW surface of cadmium iodide crystals during their aging in the air atmosphere under ambient conditions ($T = 290$ K, a relative air humidity of 80%, and an atmospheric pressure of 10^5 Pa).

2. Specimens and Experimental Technique

As described elsewhere, the layered CdI_2 single crystals were grown from the melt of a raw material preliminarily purified by the zone melting [18]. In the course of single crystal growing, thin single-crystalline CdI_2 plates were formed simultaneously from the gas phase on the walls in the upper section of an ampoule. A fresh cleavage of the crystal was obtained by removing its upper layers with the help of an adhesive tape. We also studied CdI_2 crystals grown up from the gas phase, which had a shape of plates 1 to 3 μm in thickness. The surface of those specimens was not preliminarily treated.

In order to determine the mechanism of growth of nanostructures that arise on the surface of CdI_2 crystals, the time evolution (dynamics) of their formation is studied in detail. For this purpose, the morphology

of the same region on the surface of as-cleaved crystal is investigated while keeping it in air atmosphere for 10 days.

The morphology of the crystal VdW surface was analyzed by the methods of semicontact AFM on an atomic force microscope Solver P47-PRO. The radius of a probe tip was 10 nm, and the device z-resolution equaled 1 Å.

The dimensions of the specimens did not exceed 5×5 mm^2, and their thickness varied from 0.5 to 1 mm. To prevent mechanical damages and deformations, the specimens were fixed on special substrates with the use of a bilateral adhesive tape.

To analyze the morphometric characteristics of nanostructures, a program in the Matlab environment was written. The statistical parameters were analyzed on the basis of Hoshen–Kopelman algorithm [19], which was applied to binarized digital AFM images. A linear Gauss filter and a nonlinear median one were used to remove noise from the digital AFM images.

3. Research Results

In Fig. 1, an AFM image demonstrating the morphology of the VdW surface of CdI_2 crystals grown from the gas phase and stored in the air atmosphere at room temperature ($T = 290$ K) for 30 days is shown. The analysis of obtained images allows at least three stages to be distinguished in the formation of surface nanostructures.

The first stage of the surface nanostructure formation is associated with the emergence of nanopores, which appear owing to the matrix dissolution at the outcrops of screw dislocations or other structural lattice defects (point A in Fig. 1, a). The average diameter and the depth of pores equal about 250 and 0.5 nm, respectively (point A in Fig. 1, b).

At the second stage, the surface nanoclusters in the form of cones (point B in Fig. 1, a) start to nucleate in those nanopores (a more detailed image is depicted in Fig. 1, c). The nanocluster diameter does not exceed $\sim$150 nm at this moment, its height being $\sim$5 nm (Fig. 1, d). At the third stage, the coagulation of nanostructures is observed (point C in Fig. 1, a).

In order to study the mechanism of formation of cone-shaped surface nanostructures, the kinetics of their growth during 168 h was analyzed. In Fig. 2, the AFM image of the morphology of the as-cleaved
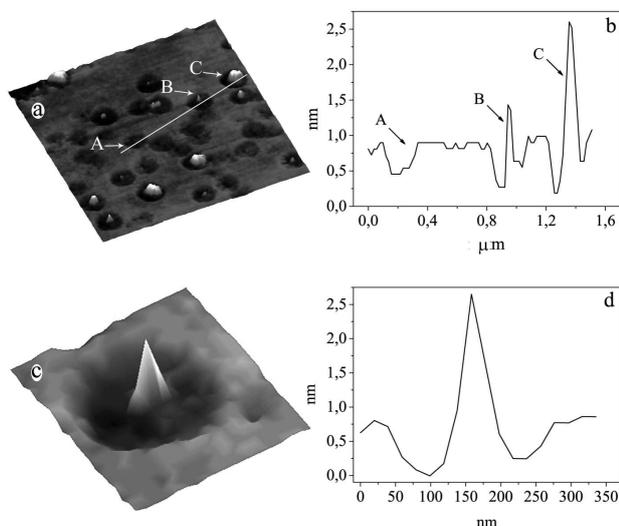
Fig. 1. AFM images of the morphology of the VdW surface of CdI$_2$ crystals grown from the gas phase and held in the air atmosphere for a long time (30 days and longer): nanostructures (A is a nanopore, and B and C are nanoclusters) (a) and their profiles (b); a nanocluster formed in a nanopore (c) and its profile (d). The images sizes are 2×2 μm^2 (a) and 320×350 nm^2 (c). The height range in (a) and (c) equals 3 nm)

VdW surface after the aging of a CdI$_2$ crystal in the air atmosphere for 1 h (this is the time interval reckoned from the cleavage formation moment to the beginning of measurements). The cone-shaped (section A in Fig. 2, a) and island (sections B_1, B_2, and B_3 in Fig. 2, a) nanostructures were formed on the CdI$_2$ surface within this time interval. Those nanostructures are different from one another not only by their shapes, but also their dimensions. The diameters and the heights of nanostructures formed on section A (Fig. 2, a) range within the intervals of 200–300 and 10–20 nm, respectively. At the same time, islands B_1, B_2, and B_3 (Fig. 2, a) are characterized by an almost doubled diameter (of about 600 nm) and a height of about 10 nm. The formation of nanostructures of another type – round troughs (C_1 and C_2 in Fig. 2, a) typical of the hexagonal atomic packing in CdI$_2$ – was observed near the island-like nanostructures. The lateral dimension of trough C$_1$ in Fig. 2, a equals about 473 nm, and its depth is about 7 nm.

A longer holding of the crystal in the air atmosphere (for 8 h) is accompanied by an increase in the lateral dimensions of troughs C_1 and C_2, and the appearance of a new trough C_3 around island B_3 (Fig. 2, b). For example, the diameter of trough
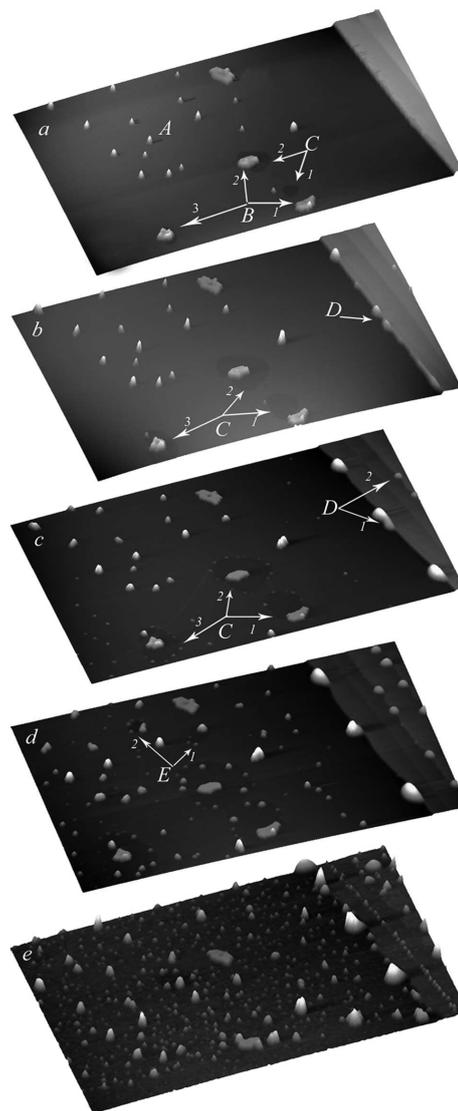

Fig. 2. Evolution of the nanostructure formation on the VdW surface of CdI$_2$ crystals grown from a melt after holding them in the air atmosphere for 1 (a), 8 (b), 24 (c), 32 (d), and 168 h (e). The size of fragments is 6×10 μm^2. The height ranges equal 34 (a), 51 (b), 55 (c), 74 (d), and 98 nm (e). A, B_1, B_2, and B_3 are nanoclusters formed on the smooth surface section; D, D_1, and D_2 are nanoclusters formed along steps. C_1, C_2, C_3, E_1, and E_2 are troughs, at the boundaries of which nanoclusters are formed

C_2 became almost twice as large and amounted to 855 nm. In addition, new nanostructures about 23 nm in height and 470 nm in diameter appeared along one of the steps (section D in Fig. 2, b).

After CdI_2 was kept in air for 24 h (Fig. 2, *c*), new nanostructures appeared at the trough boundaries (sections C_1, C_2, and C_3 in Fig. 2, *c*) and on the steps (section D_2 in Fig. 2, *c*). The height and the diameter of new nanostructures formed at the trough boundaries varied within the limits of 3–5 and 100–120 nm, respectively. In addition, the interaction between nanoformations was registered at this stage (section D_1 in Fig. 2, *c*), which gave rise to their merging with one another and to the formation of large cluster aggregates about 40 nm in height and 700 nm in diameter.

Figure 2, *d* is an AFM image of the morphology of the same CdI_2 VdW surface section after its aging in air for 32 h. There appeared new nanoclusters on the steps, and new troughs E_1 and E_2 with new nanoformations at their boundaries on the smooth surface (Fig. 2, *d*). Simultaneously, the formations emerged earlier continued their growth.

After the aging of the CdI_2 crystal in air for 7 days, an ensemble of nanostructures was formed on its VdW surface (Fig. 2, *e*). The time dependences of the dimensions of nanoclusters that were formed on the surface of CdI_2 crystal during its aging in the air atmosphere within this time interval (7 days = = 168 h) are presented in Table 1.

Table 1. **Evolution of the dimensions of cone-shaped nanostructures formed on the CdI_2 surface within a 168-h holding period in air**

No.	Cluster parameters	Holding time, h							
		8	24	32	48	54	120	144	168
1	Number	20	37	82	81	109	143	175	344
2	Minimum radius, nm	38	31	31	31	31	31	31	31
3	Maximum radius, nm	238	253	275	240	241	234	236	258
4	Average radius, nm	92	81	79	66	58	51	49	48
5	Minimum height, nm	12	4	4	9	8	8	6	6
6	Maximum height, nm	34	45	57	64	62	78	77	82
7	Average height, nm	23	20	18	23	21	23	20	18
8	Average distance between neighbor clusters, nm	922	721	474	507	434	342	309	242

The analysis of the data quoted in Table 1 shows that, during the time of observation, the rate of new nanoformation appearance exceeded the rate of their further growth. This conclusion is confirmed by the time evolution of the ratios between the minimum, maximum, and average nanostructure dimensions. The minimum radius of nanoformations almost did not change in time, the maximum radius fluctuated a little around a certain value, and the average radius demonstrated a pronounced tendency to the reduction. All those facts can be explained only if we suppose that the number of new nanoformations considerably increased. Moreover, the minimum height showed a time tendency to the reduction, the maximum one to the growth, and the average one remained almost invariable, which also can testify that the rate of new nanoformation appearance exceeded the rate of their further growth.

In order to determine the mechanism of nanoformation growth, the time variations in the dimensions of the same nanocluster within 216 h were studied (Table 2). The nanocluster height permanently grows from 15 nm during 1 h to 50 nm during 216 h with an insignificant braking at about 30 h. At the same time, the time dependence of the nanocluster radius change is more complicated. First, it grows from 66 nm during 1 h to 117 nm during 32 h, reaching the maximum; then it decreases to 76 nm during 120 h, reaching the minimum; finally, it grows again to 103 nm during 216 h. Fig. 3, *a* demonstrates the variation of the cone-shaped nanocluster volume in time, and Fig. 3, *b* the time dependence of its growth rate.

Within the time interval from 0 to 35 h (section *I* in Fig. 3, *a*), the nanocluster volume gradually increases and reaches the maximum value $V \approx 12 \times 10^{-24}$ m^3 after 35 h. However, the rate of its growth in this section has a more complicated time dependence. Namely, at the initial stage from 0 till 10 h, it decreases a little, then increases to the maximum at 25 h, and finally decreases to zero at 35 h. In the time interval from 35 to 90 h (section *II* in Fig. 3, *a*), the next stage of the nanostructure formation process is observed: this is a gradual reduction of the nanostructure volume to the minimum value $V \approx 8 \times \times 10^{-24}$ m^3. This is a section with a negative growth rate. Starting from the time moment equal to 90 h (section *III* in Fig. 3, *a*), the initial stage of the process, which was observed in the time interval from 0

to 35 h, repeats; however, the growth rate is much lower now.

Let us consider a possible mechanism of nanoformation growth in more details. As was mentioned above, the nanocluster nuclei appear on the as-cleaved crystal surface at the sites, where the surface imperfection is the largest; these are nanopores (Figs. 1, *a* and *c*). They continue to grow further following the mechanism of component interdiffusion to the reaction zone: oxygen, water, and carbon dioxide molecules (they are indicated in the decreasing order of their contents in air and their probable participation in the creation of nanoformations) arrive from the gas phase (air), and cadmium ions from the solid phase (the crystal volume). The diffusion flux of each of the indicated components to the reaction zone is described by Fick's law

$$I_i = D_i S \frac{dc_i}{dr}, \qquad (1)$$

where D_i is the diffusion coefficient of the i-th component, S the reaction zone area, and dc_i/dr the concentration gradient of the i-th component. Since the diffusion coefficients of components in the gas phase considerably exceed that of cadmium ions in the solid phase, the diffusion of the latter in the crystal volume is a process that constrains the growth of nanoclusters. The specific features of this diffusion will be responsible for general regularities in the further growth of nanoclusters.

Therefore, the growth rate of a nanocluster is governed by the magnitude of the diffusion flux of cadmium ions in the near-reaction zone:

$$\frac{dV}{dt} = I_{\text{Cd}} = D_{\text{Cd}} S \frac{dc_{\text{Cd}}}{dr}, \qquad (2)$$

where V is the nanocluster volume, and t the time of its growth. If the diffusion coefficient of cadmium ions and the reaction zone area are assumed to change little during the nanocluster growth, the corresponding growth rate will mainly be determined by the time evolution of the concentration gradient of cadmium ions in the near-reaction zone:

$$\frac{dV}{dt} \approx \frac{dc_{\text{Cd}}}{dr}. \qquad (3)$$

As one can see from Fig. 3, *b*, the growth rate of nanoclusters has a complicated time behavior, which
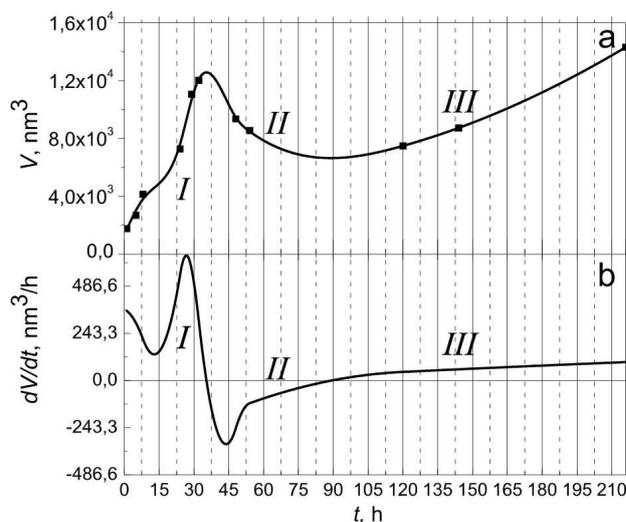
Fig. 3. Dependence of the cone-shaped nanocluster volume on the time of aging of a CdI$_2$ crystal in the air atmosphere (*a*) and the corresponding time dependence of the nanocluster growth rate (*b*)

can be explained by probable changes in the concentration gradient of cadmium ions in the near-reaction zone (Fig. 4). Let us conventionally adopt that there is a near-reaction zone between a nanocluster and the crystal volume. The concentration of cadmium ions at the boundary of this zone from the cluster surface side is always equal to zero, because cadmium ions enter

Table 2. **Size evolution of a cone-shaped nanocluster during its formation within 216 h**

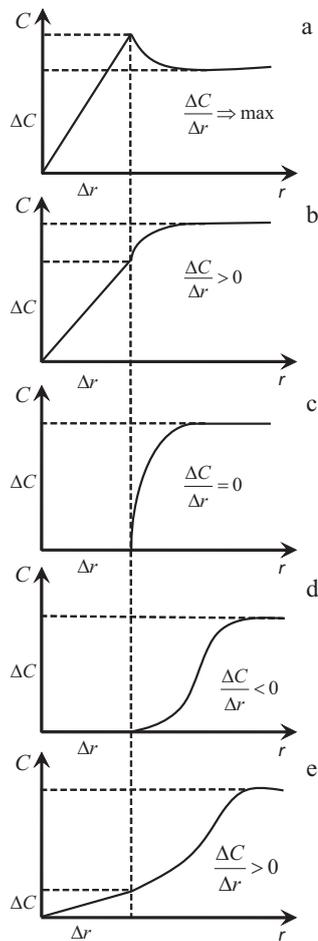| No.	Formation period, h	Cone-shaped nanocluster parameters			
		Radius, nm	Area, nm^2	Height, nm	Volume, nm^3
1	1	66	353	15	1.77×10^3
2	5	66	351	23	2.69×10^3
3	8	73	429	29	4.15×10^3
4	24	88	624	35	7.28×10^3
5	29	110	976	34	11.06×10^3
6	32	117	1093	33	12.02×10^3
7	48	88	624	45	9.36×10^3
8	54	82	546	47	8.55×10^3
9	120	76	468	48	7.49×10^3
10	144	82	546	48	8.74×10^3
11	168	85	585	49	9.56×10^3
12	216	103	859	50	14.32×10^3

Fig. 4. Changes in the concentration gradient of cadmium ions in the near-reaction zone

the nanocluster composition. At the same time, this concentration at the zone boundary from the crystal side can change from the maximum value to zero.

At the initial time moment, which corresponds to the first section in Fig. 3, *a*, the concentration gradient of cadmium ions in the near-reaction zone is maximum, because this concentration in the near-reaction zone from the crystal side can exceed the concentration of cadmium ions in the volume (iodine molecules evaporate from the wells formed on the as-cleaved surface into the gas phase, which gives rise to the growth in the surface concentration of cadmium ions (Fig. 4, *a*)). Accordingly, the growth rate of a nanocluster is high. However, it can oscillate a little within this short time interval until the equilibrium diffusion flux of cadmium ions from the crystal vol-

ume is established, which was confirmed experimentally (Fig. 3, *b*).

In the next time interval, which corresponds to the first section in Fig. 3, *b*, the concentration gradient of cadmium ions in the near-reaction zone decreases, because the cadmium ions located in the near-reaction zone from the crystal side were included into the nanocluster composition, and the other cadmium ions in the crystal volume had no time to fill their places (Fig. 4, *b*). During this period, the nanocluster formation rate diminishes from the maximum value to zero (Fig. 3, *b*). Afterward, this process continues, and the concentration of cadmium ions at the near-reaction zone boundary from the crystal side gradually decreases to zero at a certain time moment (Fig. 4, *c*). Then, the concentration gradient of cadmium ions in the near-reaction zone becomes equal to zero, so that the growth rate of nanocluster also vanishes (Fig. 3, *b*).

In the next time interval corresponding to the second section in Fig. 3, *a*, the diffusion of cadmium ions from the crystal volume does not provide their presence in the near-reaction zone from the crystal side. This deficiency is compensated by the diffusion of cadmium ions from the nanocluster to the near-reaction zone boundary and across it (Fig. 4, *d*). As a result, the volume of a nanocluster, as well as its area, should diminish, which corresponds to the section with a negative growth rate of nanoclusters in Fig. 3, *b*. This fact agrees well with experimental results, according to which the radius of nanoclusters gradually decreases from 117 to 76 nm in the time interval from 32 to 120 h, whereas their height simultaneously increases from 33 to 48 nm.

For longer times of the nanocluster formation, which correspond to the third section in Fig. 3, *a*, the diffusion of cadmium ions in the crystal volume gradually smoothed out the gradient of their concentration, and a certain equilibrium concentration of cadmium ions is established in the near-reaction zone from the crystal side, which provides the further growth of nanoclusters following the diffusion mechanism (Fig. 4, *e*). The growth rate of nanoclusters gradually increases, but it remains much lower in comparison with that in the first section (Fig. 3, *b*).

4. Conclusions

To summarize, on the basis of the results obtained by atomic force microscopy, the mechanism governing

the formation of nano-sized structures on the van der Waals surfaces of CdI$_2$ crystals during their aging in the air atmosphere under thermodynamic conditions close to the equilibrium ones is determined. The process of nanostructure formation on the surface can be divided into three stages: the first stage comprises the creation of pores owing to the matrix dissolution at the outcrops of screw dislocations or other structural defects of the lattice; cone-shaped nanoclusters emerge and grow in those pores at the second stage; finally, at the third stage, nanoclusters coagulate. Experimental results concerning the growth kinetics of cone-shaped nanoclusters are described in the framework of the proposed model, which is based on the interdiffusion of components. The complicated behavior of the rate of nanocluster growth is explained by changes in the concentration gradient of cadmium ions in the near-reaction zone.

1. K. Ueno, K. Sasaki, K. Saiki *et al.*, Jpn. J. Appl. Phys. **38**, 511 (1999).
2. S.I. Drapak, A.P. Bakhtinov, S.V. Gavrilyuk *et al.*, Fiz. Tverd. Tela **48**, 1515 (2006).
3. O. Lang, R. Schlaf, Y. Tomm *et al.*, J. Appl. Phys. **75**, 7805 (1994).
4. A.I. Dmitriev, Zh. Tekhn. Fiz. **82**, 114 (2012).
5. A.I. Dmitriev, V.V. Vishnyak, G.V. Lashkarev *et al.*, Fiz. Tverd. Tela **53**, 579 (2011).
6. A.P. Bakhtinov, Z.R. Kudrinskii, and O.S. Litvin, Fiz. Tverd. Tela **53**, 2045 (2011).
7. O.A. Balitskii, Mater. Lett. **60**, 594 (2006).
8. O.A. Balitskii, J. Electr. Microsc. **55**, 261 (2006).
9. R. Singh, S. Samanta, A. Narlikar *et al.*, J. Cryst. Growth **204**, 233 (1999).
10. R. Singh, S. Samanta, A. Narlikar *et al.*, Bull. Mater. Sci. **23**, 131 (2000).
11. B. Kumar and N. Sinha, Cryst. Res. Technol. **40**, 887 (2005).
12. R. Singh, S. Samanta, A. Narlikar *et al.*, Surf. Sci. **422**, 188 (1999).
13. N.-Y. Cui, N.M.D. Brown, and A. McKinley, Appl. Surf. Sci. **152**, 266 (1999).
14. N. Sallacan, R. Popovitz-Biro, and R. Tenne, Solid State Sci. **5**, 905 (2003).
15. I.M. Bolesta, R.I. Gritskiv, Yu.R. Datsyuk *et al.*, Ukr. Fiz. Zh. **48**, 1 (2003).
16. I.M. Bolesta, I.N. Rovetskyj, I.D. Karbovnyk *et al.*, Techn. Phys. Lett. **39**, 463 (2013).
17. Q.-J. Liu, Z.-T. Liu, and L.-P. Feng, Phys. Status Solidi B **248**, 1629 (2011).
18. *Wide-Gap Layered Crystals and Their Physical Properties*, edited by A.B. Lyskovich (Vyshcha Shkola, Lviv, 1982) (in Russian).
19. A.L. Efros, *Physics and Geometry of Disorder: Percolation Theory* (Mir Publishers, Moscow, 1986).

І.М. Болеста, І.М. Ровецький, З.М. Яремко,
І.Д. Карбовник, С.Р. Вельгош, М.В. Партика,
Н.В. Глосковська, В.М. Лесівців

ПРО МЕХАНІЗМ РОСТУ
НАНОСТРУКТУР НА ПОВЕРХНІ CdI$_2$

Р е з ю м е

Методами атомно-силової мікроскопії досліджено динаміку формування нанорозмірних структур на ван-дер-ваальсовій поверхні кристалів CdI$_2$ під час їхнього витримування в атмосфері повітря за термодинамічних умов, близьких до рівноважних. У формуванні поверхневих наноструктур виявлено три стадії: на першій утворюються нанопори через розчинення матриці у місцях виходу гвинтових дислокацій або інших структурних дефектів ґратки, на другій у цих нанопорах зароджуються конусоподібні нанокластери, які з часом збільшуються у розмірах, і на останній третій стадії вони коагулюють. Кінетика росту поверхневих конусоподібних нанокластерів описана дифузійною моделлю, яка ґрунтується на зустрічній дифузії компонентів, що входять до їхнього складу. Показано, що швидкість росту цих нанокластерів залежить від часової зміни градієнта концентрації іонів кадмію у приреакційній області.